CrossMark

ORIGINAL ARTICLE

Uptake of synthetic naked RNA by skin-resident dendritic cells via macropinocytosis allows antigen expression and induction of T-cell responses in mice

Abderraouf Selmi[1,2] · Fulvia Vascotto[1] · Kordula Kautz-Neu[3] · Özlem Türeci[4] · Ugur Sahin[1,2,5] · Esther von Stebut[3] · Mustafa Diken[1,5] · Sebastian Kreiter[1,5]

Abstract Intradermal administration of antigen-encoding RNA has entered clinical testing for cancer vaccination. However, insight into the underlying mechanism of RNA uptake, translation and antigen presentation is still limited. Utilizing pharmacologically optimized naked RNA, the dose–response kinetics revealed a rise in reporter signal with increasing RNA amounts and a prolonged RNA translation of reporter protein up to 30 days after intradermal injection. Dendritic cells (DCs) in the dermis were shown to engulf RNA, and the signal arising from the reporter RNA was significantly diminished after DC depletion. Macropinocytosis was relevant for intradermal RNA uptake and translation in vitro and in vivo. By combining intradermal RNA vaccination and inhibition of macropinocytosis, we show that effective priming of antigen-specific CD8$^+$ T-cells also relies on this uptake mechanism. This report demonstrates that direct antigen translation by dermal DCs after intradermal naked RNA vaccination is relevant for efficient priming of antigen-specific T-cells.

Keywords Naked RNA · Intradermal vaccination · Macropinocytosis · Dermal dendritic cell · RNA vaccine · Cancer immunotherapy

Abderraouf Selmi and Fulvia Vascotto have contributed equally to the first authorship. Mustafa Diken and Sebastian Kreiter have contributed equally to the last authorship.

✉ Mustafa Diken
   Mustafa.Diken@TrOn-Mainz.de

✉ Sebastian Kreiter
   Sebastian.Kreiter@TrOn-Mainz.de

1   TRON-Translational Oncology at the University Medical Center of Johannes Gutenberg University gGmbH, Freiligrathstraße 12, 55131 Mainz, Germany

2   Research Center for Immunotherapy (FZI), University Medical Center of Johannes Gutenberg University, Mainz, Germany

3   Department of Dermatology, University Medical Center of Johannes Gutenberg University, Mainz, Germany

4   Cluster for Individualized Immune Intervention (CI3), Mainz, Germany

5   BioNTech RNA Pharmaceuticals GmbH, Mainz, Germany

Abbreviations
APC   Antigen-presenting cell
DC   Dendritic cell
DT   Diphtheria toxin
DTR   Diphtheria toxin receptor
eGFP   Enhanced green fluorescent protein
HA   Hemagglutinin
IFN   Interferon
LN   Langerin
Luc   Luciferase
SEM   Standard error of mean

Introduction

The skin is a highly active immune organ containing a large population of resident antigen-presenting cells (APCs) [1]. The skin of a healthy individual is estimated to contain around 20 billion T-cells, which is nearly twice the number present in circulation [2]. T-cells and the other cellular components involved form a network of immune cells which was named the skin immune system [3]. The efficacy of this system is demonstrated by the lifelong protection conferred by intradermally administered vaccines against rabies [4].

🖄 Springer

In vitro-transcribed synthetic mRNA encoding for tumor antigens is one of the promising future vaccine formats, which is administered into the skin. This approach was explored in preclinical studies starting in the early 2000s [5] demonstrating that humoral and cellular immune responses can be induced. Clinical trials were performed in various cancer indications utilizing either naked synthetic RNA or combinations of synthetic RNA and adjuvants intradermally [6–8].

We recently gained insight into the mechanisms of uptake of RNA administered into lymph nodes which is currently in clinical testing (NCT01684241). We could show that immature dendritic cells (DCs) engulf RNA after intralymphatic injection enabling expression of encoded antigens. This uptake is mediated by macropinocytosis, a fluid-phase uptake mechanism that is constitutively active in immature DCs [9, 10]. Here, we asked the question which tissue resident cells and which mechanism contributes to the uptake of RNA administered intradermally, which would allow expansion of antigen-specific CD8$^+$ T-cells. In order to answer these questions, we employed pharmacologically optimized RNA with improved stability, translational performance, and presentation of the encoded antigen on MHC class I and II molecules [11–13].

In this study, we demonstrate direct involvement of dermal DCs in macropinocytosis-mediated RNA uptake as well as efficient priming of antigen-specific T-cells in the context of intradermal RNA vaccination.

Materials and methods

Animals

Female 8- to 12-week-old C57BL/6 mice were purchased from Janvier or Harlan Laboratories. CD11c-DTR (diphtheria toxin receptor) mice on C57BL/6 background were kindly provided by K. Steinbrink (Department of Dermatology, Johannes Gutenberg University of Mainz). All animal experiments complied with the guidelines set by the Johannes Gutenberg University of Mainz.

Synthetic peptides

Chicken ovalbumin (OVA)-derived SIINFEKL peptide (H2-Kb-restricted OVA257-264) was obtained from Jerini Peptide Technologies (JPT).

RNA constructs

pSTI-A120 and pSTI-MITD vectors were used as plasmid templates for in vitro transcription of naked antigen-encoding RNAs [12, 14]. eGFP and LUC constructs in the pST1-A120 vector backbone encode for the enhanced green fluorescence and firefly luciferase proteins, respectively. SIINFEKL and HA constructs in the pST1-MITD vector backbone encode for the immunodominant epitope (aa 257–264) of OVA and partial sequence of influenza hemagglutinin (strain A/PR/8/34; aa 60–285 fused to aa 517–527), respectively.

In vitro transcription, labeling of RNA and transfer into cells

RNA was generated by in vitro transcription as described previously [15]. HA construct was used to generate Cy5-labeled RNA using Cy5-UTP according to manufacturer's instructions (GE Healthcare). For in vitro pulsing, 1–3.10^6 cells were centrifuged and incubated with RNA in RNase-free PBS (Ambion) for 15 min in a volume of 10–20 µl followed by cultivation in the respective medium at 37 °C with 5 % CO_2. For in vitro experiments, cells were treated with rottlerin (10 µM; Calbiochem) or DMSO as control for 30 min at 37 °C prior to RNA pulsing.

Immunization of mice and de novo priming of T-cells

C57BL/6 mice anesthetized with xylazine/ketamine were injected intradermally in ear pinna or flank with 20 µg of RNA formulated in PBS or PBS only as control using a single-use 0.3-ml syringe with an ultrafine needle (31G, Becton–Dickinson). For CD8$^+$ T-cell de novo priming, four intradermal immunizations of SIINFEKL-RNA on days 0, 3, 7 and 11 were performed into the right or left ear pinna of mice using alternate injections.

Cell isolation from mouse ears

Ears were excised, soaked in 70 % ethanol and washed with PBS. The ears were split into halves and incubated in 0.4 mg/ml liberase (Sigma-Aldrich) in RPMI 1640 with penicillin (500 U/ml)/streptomycin (500 µg/ml; gibco Life Technologies) for 1.5 h at 37 °C. Reaction was inactivated by adding complete RPMI 1640 containing 5 % FCS, and cell suspension was incubated in Medicon chamber (Medimachine, BD) for 7 min for the disaggregation of the tissue. Next, cell suspensions were mashed through a 70-µm-pore size filter and centrifuged at 200g for 8 min. Cells were resuspended in PBS for flow cytometry analysis.

Isolation of epidermal and dermal cell suspensions

Ear skin was trypsinized with 0.5 % trypsin (GE Healthcare) in HBSS (BioWhittaker) for 30 min at 37 °C followed by gentle pipetting in HBSS containing 0.05 % DNase (Sigma-Aldrich) and 30 % FCS to retrieve the epidermal

cells from dissociated epidermal sheets. Cells were then filtered through a 70-μm nylon mesh. After removal of the epidermis, dermal cell suspensions were prepared by mincing the dermal tissue into small pieces and their incubation for 2 h at 37 °C with a solution of HBSS containing 0.1 % collagenase (Sigma-Aldrich), 0.05 % DNase and 2 % FCS. Epidermal and dermal cells were identified by expression of CD11c, CD24 and EpCam (Langerhans cells: CD11c$^+$CD24$^+$EpCam$^+$; Langerin (LN)$^-$ dermal DCs: CD11c$^+$CD24$^-$; and LN$^+$ dermal DCs: CD11c$^+$CD24$^+$EpCam$^-$).

Depletion of CD11c$^+$ DCs in CD11c-DTR mice

CD11c-DTR mice were injected i.p. with 4–8 ng of diphtheria toxin (DT)/g (Sigma-Aldrich) of body weight dissolved in PBS at days 0 and 1. PBS-treated groups served as controls.

Antibodies and flow cytometry analysis

For analysis of skin DCs, the following antibodies were used: Pacific Blue anti-mouse MHCII (M5/114.15.2; BioLegend), FITC anti-mouse CD11c (HL3; BD), PE anti-mouse CD11c (HL3; BD), PE anti-mouse CD24 (M1/69; BD), PeCy7 anti-mouse CD326 (EpCam; clone G8.8; e-Bioscience) and APC anti-mouse F4/80 (BM8; BD). MHC-peptide tetramer staining from blood and spleen samples was performed with H-2 Kb/SIINFEKL tetramer (Beckman Coulter) and CD8 antibody (Invitrogen). Flow cytometry data were acquired using FACS Calibur or LSRII flow cytometer (BD) and analyzed by FlowJo software (Tree Star).

ELISPOT assay

5×10^5 spleen cells/well were pulsed with peptide (2 μg/ml) in microtiter plates coated with an anti-interferon (IFN)-γ antibody (10 μg/ml; clone AN18, Mabtech). After 18-h incubation at 37 °C, IFN-γ secretion was detected with an anti-IFN-γ antibody (clone R4-6A2, Mabtech) as described previously [9].

Ex vivo luciferase assay

Single-cell suspensions from ears of mice were used for luminescence assay as previously described [10]. Briefly, $1–5 \times 10^6$ cells/100 μl were plated in 96-well Nunc white plates (Thermo Scientific), and 100 μl Bright-Glo luciferin reagent (Promega) was added to the cell suspension. After 3-min incubation with gentle shaking, bioluminescence counts were measured with an Infinite M200 plate reader (Tecan) for 1 s.

In vivo bioluminescence imaging

Uptake and translation of Luc-RNA were evaluated by in vivo bioluminescence imaging using the Xenogen IVIS Spectrum imaging system (Caliper Life Sciences) as previously described [10]. D-luciferin (75 mg/kg body weight; Perkin-Elmer) dissolved in PBS was injected intraperitoneally at indicated time points after administration of LUC-RNA; 5 min after luciferin injection, emitted photons from live animals were measured for 1 min. Regions of interest (ROIs) from were determined at the injection area, and bioluminescence was quantified as total radiance (photons/s) using IVIS Living Image 4.0 Software.

Immunofluorescence

Eight-μm sections of cryo-conserved ears treated with eGFP-RNA or PBS as a control were attached on Superfrost slides, dried overnight at room temperature (RT) and fixed in 4 % paraformaldehyde (PFA) for 10 min at RT in the dark. Sections were washed 3 times with PBS and blocked using PBS supplemented with 1 % BSA, 5 % mouse serum, 5 % rat serum and 0.02 % Nonidet for 1 h at room temperature in the dark. Sections were stained using Alexa 488 labeled anti-eGFP antibody (ThermoFisher) over night at 4 °C. After washing twice with washing buffer (PBS supplemented with 1 % BSA and 0.02 % Nonidet) and once with PBS, slides were stained for 3 min with Hoechst (Sigma), washed 3 times with PBS, once with distilled water and mounted using mounting medium Fluoromount G (eBioscience). Immunofluorescence images were acquired using an epifluorescence microscope (ApoTome, Zeiss).

Statistics

Statistical analysis was performed by GraphPad Prism 4 software (Graphpad Software) employing unpaired two-tailed Student's t test and one-way or two-way ANOVA test with Bonferroni's multiple comparison test. p values are provided where applicable and data are displayed as mean + SEM.

Results

To characterize the potential of synthetic RNA in inducing CD8$^+$ T-cell priming and expansion, naïve C57BL/6 mice were repetitively immunized with pharmacologically optimized RNA encoding the SIINFEKL epitope of chicken ovalbumin. To ensure that the results are not influenced by the anatomical site, we injected the vaccine intradermally in the ear pinna as well as in the flank (Fig. 1a). Five days
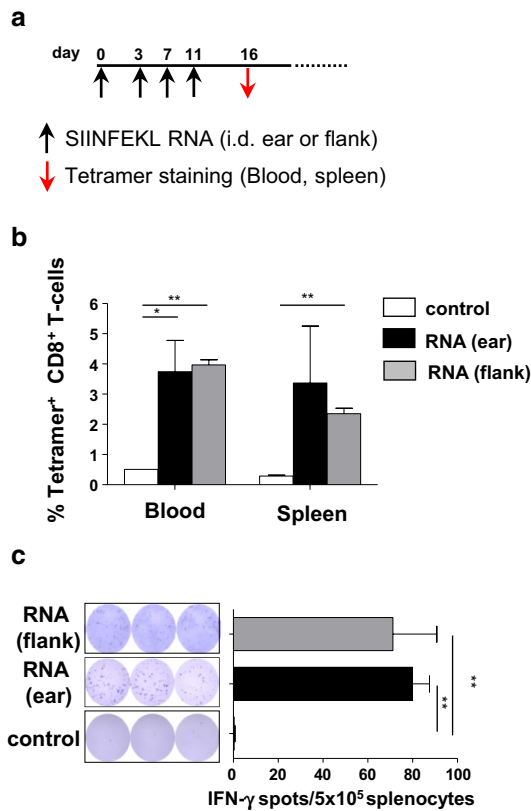
a

day 0 3 7 11 16 ....

↑ SIINFEKL RNA (i.d. ear or flank)

↓ Tetramer staining (Blood, spleen)

b

c

Fig. 1 Intradermal RNA vaccination induces antigen-specific T-cell expansion. **a** Experimental setting. C57BL/6 mice ($n = 5$) were immunized intradermally (i.d.) in the ear pinna (ear) or in the flank with SIINFEKL-RNA (20 µg) on day 0, 3, 7 and 11 or left untreated as control. **b** Frequencies of SIINFEKL-specific CD8^{+} T-cells were assessed via tetramer staining in the peripheral blood and spleen of treated mice 5 days after the last immunization. **c** SIINFEKL-specific CD8^{+} T-cell response was analyzed in spleen by IFN-γ ELISPOT assay 5 days after the last immunization. *Bars* represent mean + SEM, *$p < 0.05$, **$p < 0.01$, one-way ANOVA test

after the last vaccination, the epitope-specific T-cell frequency was determined by MHC-tetramer as well as IFN-γ ELISPOT assay. The induction of the immune responses was robust, resulting in frequencies of around 3–4 % of SIINFEKL-specific CD8^{+} T-cells among total CD8^{+} T-cells assessed via the tetramer staining in the peripheral blood and spleen (Fig. 1b). In line with this, vaccination at both sites induced similar frequencies of IFN-γ secreting antigen-specific CD8^{+} T-cells as revealed by IFN-γ ELISPOT assay (Fig. 1c). Indeed, no significant differences were observed between the different vaccination sites ruling out that the anatomical site of the ear pinna is responsible for the effects observed. Further studies were therefore performed with the accepted gold-standard intra-pinna injection allowing maximum control for intradermal application of the fluid.

The establishment of a dose–response relationship is an important step for the vaccine development. In the field of RNA vaccination, an accepted parameter predicting epitope density on the surface of APCs is the kinetics of the translated protein. Utilizing the firefly luciferase-encoding RNA (Luc-RNA) and in vivo bioluminescence imaging, we characterized the dose and time kinetics after intradermal injection of optimized RNA. Interestingly, we observed a linear dose–response for RNA amounts from 1 up to 20 µg and the signal of the RNA-encoded luciferase (Fig. 2a). Another important parameter affecting the total amount of translated protein is the time kinetics of translation. After intradermal injection of 20 µg Luc-RNA, we observed an signal increase from 2 up to 6 h post-injection, followed by a prolonged expression at plateau until day 3 (Fig. 2b, c). Surprisingly, we were able to measure signal above background for 30 days proving the translational efficacy of the optimized RNA used. Again, we investigated the influence of the injection site by measuring the time kinetic in the flank as well as the ear pinna, which showed slightly faster signal decay in the flank (Fig. 2d).

After characterizing relevant pharmacological parameters for optimized synthetic RNA, we asked whether we could define in more detail the origin of the signal in the skin tissue. We first explored whether the epidermis or the dermis would differ in RNA uptake. For this purpose, the epidermal and dermal sheets separated after intradermal injection of Luc-RNA were quantified using an ex vivo luciferase assay. Interestingly, the signal was observed predominantly in cells originated from the dermis (Fig. 3a). Utilizing eGFP-encoding RNA, this observation could be validated in the cryosections of the ear pinna (Fig. 3b). Moving from the analysis of different localization to the subsets of cells, we employed Cy5-labeled RNA for the flow cytometric characterization of different cell types transfected in the skin. We found no relevant signal in the epidermis (Fig. 3c), whereas the dermal dendritic cells (DCs) and macrophages (F4-80^{+} cells) exhibited a positive signal. Dissecting the DC populations further, we found that LN[+] dermal and LN[−] dermal DCs were the main RNA-transfected dermal DC populations (Fig. 3c right panel). Finally, it was important to provide functional evidence for DC involvement in RNA uptake and translation. This was studied by making use of the CD11c-DTR mouse model [16], which allows temporal DC depletion after application of DT. As expected, we observed a significant bioluminescence signal reduction in mice after depletion of DCs, to one-third of the signal obtained in control mice (Fig. 3d). However, in these mice residual luciferase signal still can be detected in the ear due to the incomplete depletion of dermal DCs by the DT (data not shown).
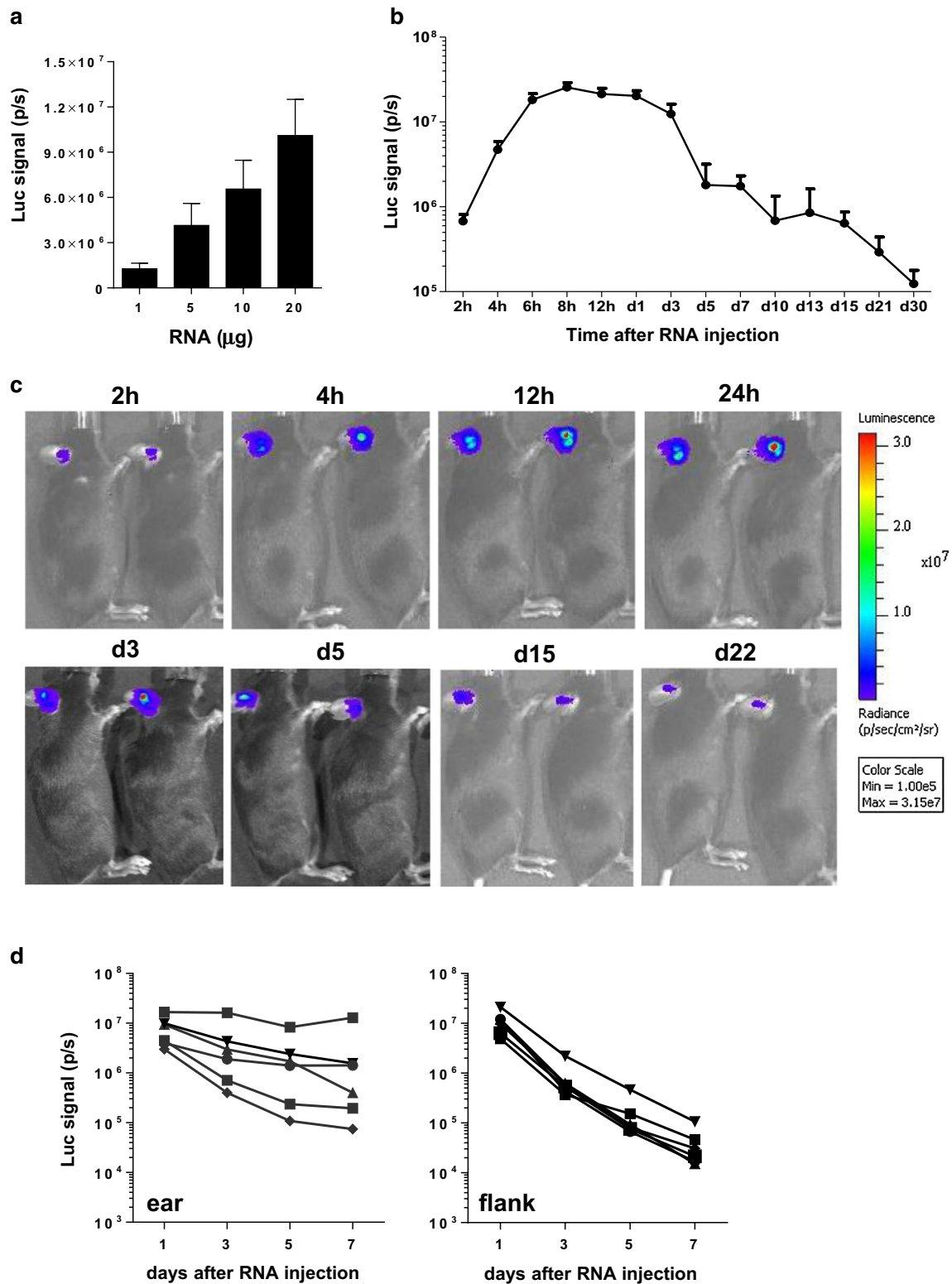
Fig. 2 RNA expression in skin is dose dependent and sustained in time utilizing optimized RNA constructs. **a** C57Bl/6 mice ($n = 3$) received intradermal (ear) different doses (1, 5, 10 and 20 µg) of RNA encoding for luciferase (Luc-RNA). Translation of Luc-RNA was evaluated by in vivo bioluminescence imaging 24 h later. **b** C57Bl/6 mice ($n = 3$) received i.d (ear) Luc-RNA (20 µg) and luciferase expression was monitored by in vivo bioluminescence. **c** Representative mice are shown. **d** Comparison of luciferase expression over the time after intradermal injection of Luc-RNA (20 µg) into the ear pinna or the flank of C57Bl/6 mice ($n = 6$)
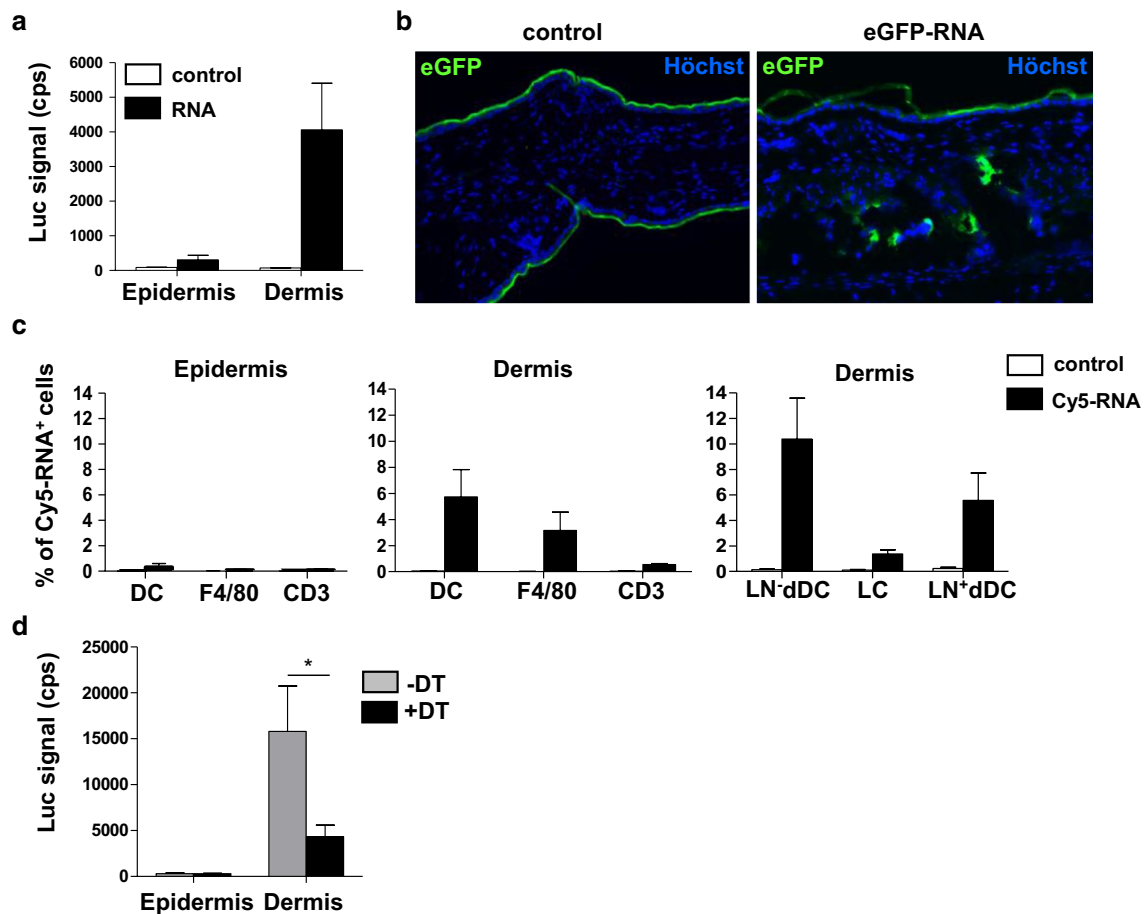
Fig. 3 Translation of the RNA-encoded protein is confined to dermis. **a** C57Bl/6 mice ($n = 3$) received i.d (ear) Luc-RNA (20 µg) or buffer as control. Epidermal and dermal sheets were isolated and enzymatically digested. *Ex vivo* luminescence was measured. **b** C57Bl/6 mice ($n = 3$) received i.d (ear) GFP-RNA (20 µg) or buffer as control. After 24 h, ears were cryoconserved for immunfluorescence analysis. **c** C57Bl/6 mice ($n = 3$) received i.d (ear) Cy5 labeled RNA (20 µg) or buffer as control. Epidermal and dermal sheets were isolated and enzymatically digested, and cells were used for flow cytometry. *Graphs* indicate % of Cy5+ cells in each indicated population. **d** C57Bl/6 CD11c-DTR transgene mice ($n = 3$) were treated with 4–8 ng/g of body weight diphtheria toxin (+DT) or buffer (−DT) i.p. on d0 and d1. On d2, mice received i.d (ear) Luc-RNA (20 µg). Epidermal and dermal sheets were isolated and enzymatically digested, and cells were used for ex vivo luminescence assay. *Bars* represent mean + SEM, *$p < 0.05$, unpaired t test

As we had already demonstrated that the inhibition of macropinocytosis abrogates RNA engulfment by DCs in vitro and in vivo upon intranodal injection [10], we hypothesized that this mechanism might also apply to dermal DCs. Employing rottlerin as a macropinocytosis inhibitor, we first investigated its effect on RNA uptake in vitro using a single-cell suspension obtained from skin. The cells were treated with rottlerin or the vehicle and thereafter pulsed with Luc-RNA. The luminescence assay performed 24 h after RNA pulsing showed a strong reduction in the luciferase signal in rottlerin-treated cells due to the weaker RNA uptake by DCs (Fig. 4a). To rule out that the observed phenomenon is attributable only to in vitro conditions, we also adopted the same setting in an in vivo experiment. After treatment of the skin with intradermal rottlerin injection, Luc-RNA was injected intradermally and the

bioluminescence signal was measured 4, 8 or 24 h later. In line with the in vitro data described above, the luciferase signal was strongly reduced in the rottlerin pre-treated group (Fig. 4b, c) fitting to the hypothesis that luciferase expression by dermal DCs count on the RNA uptake by macropinocytosis.

We then asked whether direct RNA uptake by dermal DCs after intradermal RNA vaccination is relevant for the induction of T-cell immunity. To this end, we combined the setting of intradermal rottlerin pre-treatment as described above before each of the four vaccinations using SIINFEKL-encoding RNA (Fig. 5a). Interestingly, the quantification of the immune response 5 days after the last vaccination revealed a high frequency of SIINFEKL-specific CD8+ T-cells with a good effector function, which were strongly diminished in the rottlerin pre-treated group (Fig. 5b–d).
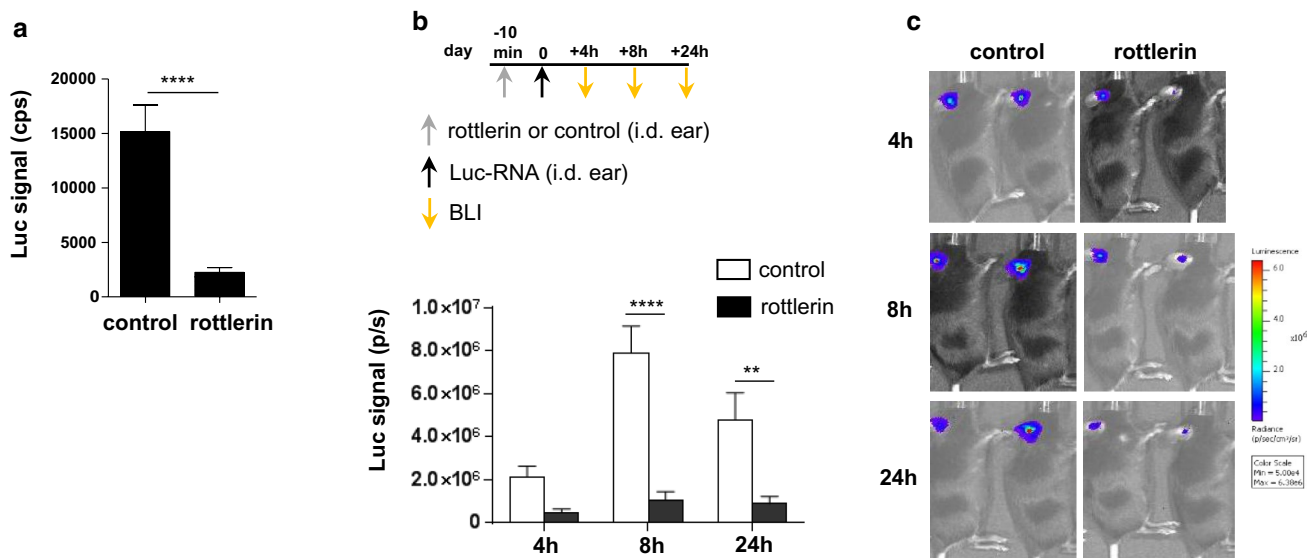
Fig. 4 Macropinocytosis is relevant for RNA uptake in vitro and in vivo. **a** Cells suspensions from the ears of C57Bl/6 mice ($n = 3$) treated for 30 min with rottlerin (10 μM) or vehicle (DMSO) as control were pulsed ex vivo with Luc-RNA, and bioluminescence flux was measured. *Bar* represents mean + SEM, ****$p < 0.0001$, unpaired *t* test. **b** Experimental setting. C57Bl/6 mice ($n = 3$) were treated i.d (ear) with rottlerin (10 μM) or vehicle (DMSO) as control, 10 min prior to intradermal injection of Luc-RNA (20 μg), and in vivo bioluminescence was monitored at 4, 8 and 24 h after injection. *Bars* represent mean + SEM, **$p < 0.01$, ****$p < 0.0001$ + SEM, two-way ANOVA test. **c** Representative bioluminescent *images* of mice are shown

These results prove that antigen translation in dermal DCs after intradermal RNA vaccination is relevant for the priming of antigen-specific T-cells thanks to the efficient antigen processing and presentation by the transfected DCs.

Discussion

Direct vaccination with naked antigen-encoding RNA against cancer obviates the need for the laborious ex vivo generation as well as transfer of RNA-transfected DCs and is therefore regarded as a promising strategy which entered into clinical setting [17]. Intradermal administration is yet a frequently used feasible route for introduction of RNA into APCs resident in the skin. Although various preclinical and clinical T-cell responses were observed upon intradermal administration of RNA, surprisingly few data exist for the kinetics of protein expression, the cell type internalizing RNA and the underlying mechanism of RNA uptake. The only study to date hypothesized a saturable Ca^+-dependent process without defining the exact mechanism and nature of the cells responsible for RNA internalization [18]. Utilizing RNA-encoded reporter proteins and model antigens, we aimed in this study to identify these factors which in turn play important roles for the induction of T-cell responses upon intradermal RNA administration.

When we first investigated the kinetics of protein expression after RNA injection, we obtained linear increase

in the protein expression up to 20 μg injected dose of RNA, which differs from the previous observation made by Probst et al. [18]. Although the authors also found a linear increase in luciferase expression, this was only from 1 up to 5 μg of RNA, and for higher RNA amounts (up to 80 μg RNA), the maximum amount tested in that study, the signal was saturated. In our experience, we could observe persistence of luciferase signal up to 30 days, while data from the literature so far showed signal between 3 and 9 days [18, 19] indicating the potency of our pharmacologically optimized RNA. The RNAs utilized in our studies so far differ mainly in the stabilizing elements (e.g., cap analog, 5′- and 3′-UTR, poly-A-tail, antigen routing sequences. Further studies might show whether higher amounts of such optimized RNA will allow further gain in dermal protein translation. Interestingly, when investigating the signal decay kinetics upon intradermal injection of Luc-RNA into two different anatomical sites, ear pinna and flank, we observed a faster decay in the latter. The reason for these differences might be found in the distinct cellular and structural composition of the two skin loci although as discussed above it did not translate into different T-cell responses.

By using fluorescently labeled RNA and flow cytometry, we could further show for the first time that upon intradermal RNA injection in mice, dermal DCs are the main population in the dermis internalizing the RNA. As earlier investigations were restricted to the histological analyses that lack the sensitivity and quantitative throughput of flow
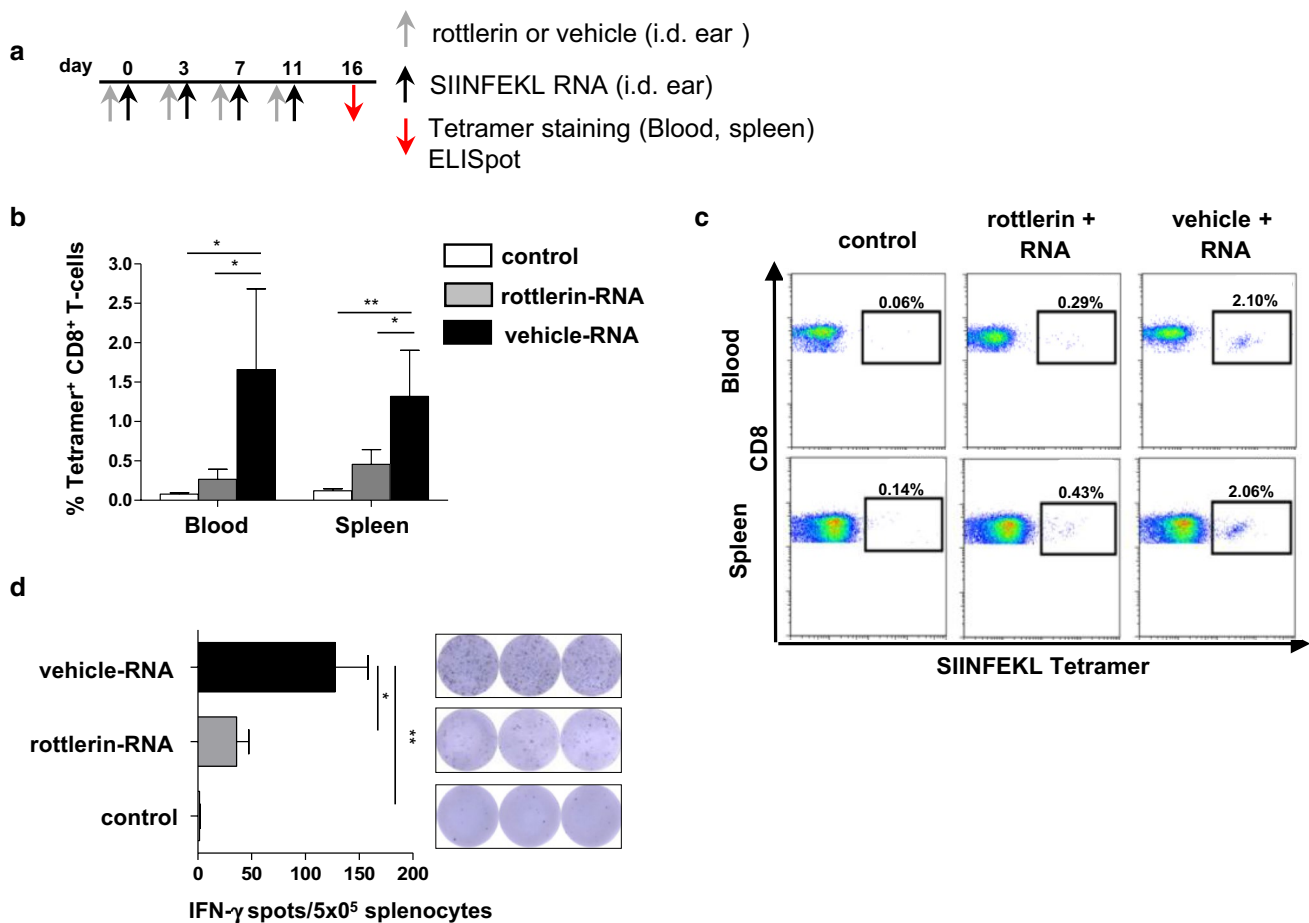
Fig. 5 Efficient T-cell priming relies on uptake of RNA via macropinocytosis. **a** Experimental setting. C57BL/6 mice ($n = 5$) were injected i.d. with rottlerin (10 μM) or vehicle (DMSO) into ear pinna 10 min prior to injection of SIINFEKL-RNA (20 μg) on day 0, 3, 7 and 11 or untreated as control. **b** Frequencies of SIINFEKL-specific CD8^{+} T-cells were assessed via tetramer staining in the peripheral blood and spleen 5 days after the last RNA immunization. **c** Representative FACS plots were shown. **d** SIINFEKL-specific CD8^{+} T-cell response in spleen was analyzed by IFN-γ ELISPOT assay 5 days after the last RNA immunization. *Bars* represent mean + SEM, *$p < 0.05$, one-way ANOVA test

cytometry, they were most probably not able to analyze the skin DC subsets in detail [18, 20]. Moreover, we could pinpoint the mechanism of RNA uptake as macropinocytosis by making use of the macropinocytosis inhibitor rottlerin. In line with previous findings that macropinocytosis is involved in the uptake of intranodally administered naked RNA by lymph node-resident DCs [10], blockage of this mechanism not only led to severe decrease in uptake but also significantly abrogated the induction of antigen-specific T-cell responses in the intradermal setting. Prior attempts reported in the literature to define the mechanism might have been failed due to the use of toxic or unspecific inhibitors of uptake [18].

Our data demonstrate that pharmacologically optimized RNA constructs administered intradermally enable sustained translation and efficient T-cell priming. Dermal DCs were identified for the first time as the main DC population

in the skin involved in RNA uptake in this setting. Furthermore, RNA uptake by dermal DCs via macropinocytosis is revealed as a key step in the induction of T-cell responses. Approaches augmenting this uptake mechanism could serve to potentiate intradermal RNA vaccination against cancer.

Compliance with ethical standards

References

1. Glenn GM, Kenney RT (2006) Mass vaccination: solutions in the skin. Curr Top Microbiol Immunol 304:247–268

2. Di Meglio P, Perera GK, Nestle FO (2011) The multitasking organ: recent insights into skin immune function. Immunity 35:857–869

3. Bos JD, Kapsenberg ML (1986) The skin immune system Its cellular constituents and their interactions. Immunol Today 7:235–240

4. Madhusudana SN, Mani RS (2014) Intradermal vaccination for rabies prophylaxis: conceptualization, evolution, present status and future. Expert Rev Vaccines 13:641–655

5. Pascolo S (2004) Messenger RNA-based vaccines. Expert Opin Biol Ther 4:1285–1294

6. Weide B, Carralot JP, Reese A, Scheel B, Eigentler TK, Hoerr I, Rammensee HG, Garbe C, Pascolo S (2008) Results of the first phase I/II clinical vaccination trial with direct injection of mRNA. J Immunother 31:180–188

7. Weide B, Pascolo S, Scheel B, Derhovanessian E, Pflugfelder A, Eigentler TK, Pawelec G, Hoerr I, Rammensee HG, Garbe C (2009) Direct injection of protamine-protected mRNA: results of a phase 1/2 vaccination trial in metastatic melanoma patients. J Immunother 32:498–507

8. Rittig SM, Haentschel M, Weimer KJ, Heine A, Muller MR, Brugger W, Horger MS, Maksimovic O, Stenzl A, Hoerr I, Rammensee HG, Holderried TA, Kanz L, Pascolo S, Brossart P (2011) Intradermal vaccinations with RNA coding for TAA generate CD8+ and CD4+ immune responses and induce clinical benefit in vaccinated patients. Mol Ther 19:990–999

9. Kreiter S, Selmi A, Diken M, Koslowski M, Britten CM, Huber C, Tureci O, Sahin U (2010) Intranodal vaccination with naked antigen-encoding RNA elicits potent prophylactic and therapeutic antitumoral immunity. Cancer Res 70:9031–9040

10. Diken M, Kreiter S, Selmi A, Britten CM, Huber C, Tureci O, Sahin U (2011) Selective uptake of naked vaccine RNA by dendritic cells is driven by macropinocytosis and abrogated upon DC maturation. Gene Ther 18:702–708

11. Vallazza B, Petri S, Poleganov MA, Eberle F, Kuhn AN, Sahin U (2015) Recombinant messenger RNA technology and its application in cancer immunotherapy, transcript replacement therapies, pluripotent stem cell induction, and beyond. Wiley Interdiscip Rev RNA 6:471–499. doi:10.1002/wrna.1288

12. Kreiter S, Selmi A, Diken M, Sebastian M, Osterloh P, Schild H, Huber C, Tureci O, Sahin U (2008) Increased antigen presentation efficiency by coupling antigens to MHC class I trafficking signals. J Immunol 180:309–318

13. Kuhn AN, Diken M, Kreiter S, Vallazza B, Tureci O, Sahin U (2011) Determinants of intracellular RNA pharmacokinetics: implications for RNA-based immunotherapeutics. RNA Biol 8:35–43

14. Holtkamp S, Kreiter S, Selmi A, Simon P, Koslowski M, Huber C, Tureci O, Sahin U (2006) Modification of antigen-encoding RNA increases stability, translational efficacy, and T-cell stimulatory capacity of dendritic cells. Blood 108:4009–4017

15. Kreiter S, Konrad T, Sester M, Huber C, Tureci O, Sahin U (2007) Simultaneous ex vivo quantification of antigen-specific CD4+ and CD8+ T cell responses using in vitro transcribed RNA. Cancer Immunol Immunother 56:1577–1587

16. Jung S, Unutmaz D, Wong P, Sano G, De los Santos K, Sparwasser T, Wu S, Vuthoori S, Ko K, Zavala F, Pamer EG, Littman DR, Lang RA (2002) In vivo depletion of CD11c+ dendritic cells abrogates priming of CD8+ T cells by exogenous cell-associated antigens. Immunity 17:211–220

17. Kreiter S, Diken M, Selmi A, Tureci O, Sahin U (2011) Tumor vaccination using messenger RNA: prospects of a future therapy. Curr Opin Immunol 23:399–406

18. Probst J, Weide B, Scheel B, Pichler BJ, Hoerr I, Rammensee HG, Pascolo S (2007) Spontaneous cellular uptake of exogenous messenger RNA in vivo is nucleic acid-specific, saturable and ion dependent. Gene Ther 14:1175–1180

19. Schlake T, Thess A, Fotin-Mleczek M, Kallen KJ (2012) Developing mRNA-vaccine technologies. RNA Biol 9:1319–1330

20. Carralot JP, Probst J, Hoerr I, Scheel B, Teufel R, Jung G, Rammensee HG, Pascolo S (2004) Polarization of immunity induced by direct injection of naked sequence-stabilized mRNA vaccines. Cell Mol Life Sci 61:2418–2424